MOLECULAR AND CELLULAR BIOLOGY, Dec. 2004, p. 10406–10415 Vol. 24, No. 23
0270-7306/04/$08.00+0 DOI: 10.1128/MCB.24.23.10406–10415.2004

Genetic Interaction between *Rb* and K-*ras* in the Control of Differentiation and Tumor Suppression

Chiaki Takahashi,[1,2,3] Bernardo Contreras,[1,2] Roderick T. Bronson,[4,5] Massimo Loda,[1,6] and Mark E. Ewen[1,2]*

Department of Medical Oncology, Dana Farber Cancer Institute,[1] Department of Medicine,[2] Rodent Histopathology Core,[5] and Department of Pathology,[6] Harvard Medical School, and Department of Pathology, Tufts University Schools of Medicine and Veterinary Medicine,[4] Boston, Massachusetts, and Department of Molecular Oncology and 21st Century Center of Excellence, Kyoto University Graduate School of Medicine, Kyoto, Japan[3]

Received 12 April 2004/Returned for modification 21 May 2004/Accepted 2 September 2004

Although the retinoblastoma protein (pRb) has been implicated in the processes of cellular differentiation, there is no compelling genetic or in vivo evidence that such activities contribute to pRb-mediated tumor suppression. Motivated by cell culture studies suggesting that Ras is a downstream effector of pRb in the control of differentiation, we have examined the tumor and developmental phenotypes of *Rb* and K-*ras* double-knockout mice. We find that heterozygosity for K-*ras* (i) rescued a unique subset of developmental defects that characterize *Rb*-deficient embryos by affecting differentiation but not proliferation and (ii) significantly enhanced the degree of differentiation of pituitary adenocarcinomas arising in *Rb* heterozygotes, leading to their prolonged survival. These observations suggest that *Rb* and K-*ras* function together in vivo, in the contexts of both embryonic and tumor development, and that the ability to affect differentiation is a major facet of the tumor suppressor function of pRb.

Inheritance of a mutated allele of the retinoblastoma gene (*Rb*) predisposes to familial retinoblastoma, and *Rb* is also frequently inactivated in sporadic human cancers of diverse histological origins (10). Mice heterozygous for *Rb* develop pituitary adenocarcinomas and thyroid adenomas (13–15, 44), suggesting that the mouse can be used to understand the pathways through which *Rb* exerts its tumor suppressor functions. Further, nullizygosity for *Rb* results in lethality at midgestation, with embryos displaying defects in proliferation and differentiation (5, 15, 21, 47). Thus, the combined analysis of $Rb^{+/-}$ and $Rb^{-/-}$ mice provides an opportunity to dissect the functions of the retinoblastoma protein (pRb) that contribute to its tumor suppressor functions.

pRb is best characterized for its role in controlling proliferation; this is accomplished through its regulated interaction with the E2F family of transcription factors (9). The significance of pRb-mediated inhibition of proliferation through E2F has been analyzed in the mouse. $Rb^{-/-}$ embryos display cell-autonomous deregulated proliferation in tissues such as the central nervous system (CNS) and lens (7, 25, 45), and compound embryos lacking *Rb* and *E2f1*, *E2f2*, or *E2f3* show reduced levels of ectopic DNA replication in these tissues (33, 41, 49). Mirroring the effects seen during embryonic development, loss of *E2f1* or *E2f3* significantly reduced the frequency of grossly detectable pituitary tumors (46, 48), suggesting that deregulated proliferation, mediated by *E2f*, contributes to tumor formation following loss of *Rb*.

Cell culture-based experiments suggest that pRb also participates in several differentiation programs such as adipogenesis (3, 6), osteogenesis (34, 40), and myogenesis (11, 27). A role for *Rb* in skeletal muscle differentiation in the mouse has also been demonstrated (47). The available evidence suggests that pRb regulates differentiation by influencing the activity of a number of differentiation-promoting transcription factors such as MyoD (11, 27, 28), the glucocorticoid receptor (35, 36), C/EBPβ (2–4), and CBFA1 (40). The potential clinical importance of these observations is suggested by the identification of naturally occurring *Rb* mutants whose protein products fail to interact with E2F, yet which maintain the ability to promote differentiation (19, 34). However, whether the ability of pRb to promote differentiation participates in tumor suppression has not been tested.

Cell culture-based experiments have suggested that Ras is a downstream effector of pRb in the control of cellular differentiation. Nullizygosity for the retinoblastoma gene (*Rb*) or inactivation of pRb by simian virus 40 T antigen in murine fibroblasts results in aberrantly elevated Ras and mitogen-activated protein kinase (MAPK) activity (22, 31). And the effect of *Rb* loss on Ras has been linked to a failure in differentiation. Inhibition of Ras in *Rb*-deficient myoblasts significantly potentiates the activity of MyoD and the expression of a marker of muscle differentiation (22). Similarly, the activity of the glucocorticoid receptor is restored by inhibition of Ras activity in $Rb^{-/-}$ fibroblasts (22). These findings are in keeping with the observation that oncogenic Ras possesses the ability to block the activity of these transcription factors. Additionally, inhibition of the elevated MAPK activity in *Rb*-deficient mouse embryonic fibroblasts (MEFs) restores their ability to undergo adipogenesis (12). These studies suggest that pRb antagonizes Ras signaling during differentiation.

Here we have investigated the requirement for K-*ras* function in developmental defects and tumor formation caused by loss of *Rb*. We find that heterozygosity for K-*ras* reverses many of the differentiation defects observed in *Rb*-deficient embryos.

* Corresponding author. Mailing address: Dana-Farber Cancer Institute, 44 Binney St., Boston, MA 02115. Phone: (617) 632-2206. Fax: (617) 632-5417. E-mail: mark_ewen@dfci.harvard.edu.

In addition, pituitary tumors arising in *Rb* K-*ras* heterozygotes are more differentiated than those in $Rb^{+/-}$ mice. These findings link the ability of *Rb* to positively influence differentiation to its tumor suppressor function.

MATERIALS AND METHODS

Generation of mice and embryos. Parental $Rb^{+/-}$ (15) and K-$ras^{+/-}$ (16) mice were maintained on a mixed C57BL/6 × 129/Sv genetic background and intercrossed. From the subsequent founders, $Rb^{+/-}$ K-$ras^{+/-}$ females were crossed with $Rb^{+/-}$ K-$ras^{+/-}$ males for both timed pregnancies and the generation of a cohort of adult mice. Timed pregnancies were established by the detection of a plug, taken as embryonic day 0.5 (E0.5). Mice and embryos were genotyped by PCR of genomic DNA extracted from tails and yolk sacs, respectively, as previously described (15, 16). All animal experiments were performed at the Dana-Farber Cancer Institute Animal Resource Facility in accordance with the guidelines of the National Institutes of Health.

Histology and immunohistochemistry. Embryos were fixed in 4% paraformaldehyde–phosphate buffered saline (PBS, pH 7.4) for 12 h, preserved in 70% ethanol for 5 days with occasional changes of buffer, and embedded in paraffin for sectioning. Sections (thickness, 6 μm) were stained with hematoxylin and eosin (H&E). Unstained sections were incubated with a monoclonal antibody (MY-32; Sigma) to myosin heavy chain (MHC) following deparaffinization and rehydration. To identify proliferating cells, 50 μg of 5-bromodeoxyuridine (BrdU)/g of body weight was injected intraperitoneally into pregnant mice 1 h prior to sacrifice. Sections were treated with 0.05 mM trypsin–2 N HCl in PBS (pH 6.0), blocked with 6% goat serum, and incubated with an anti-BrdU monoclonal antibody (B44; Becton Dickinson) in the presence of 0.5% Tween 20 in PBS (pH 7.4). The bound primary antibody (anti-MHC or anti-BrdU) was detected with the ABC mouse peroxidase detection system (Santa Cruz Biotechnology). For analysis of cell death, embryos were fixed in formalin (3.7% formaldehyde in PBS), from which tissue sections were generated. Apoptosis was measured by a terminal deoxynucleotidyltransferase-mediated dUTP-biotin nick end labeling (TUNEL) assay using the ApopTag mouse peroxidase plus system (Intergen). Adult animals were fixed in Bouin's solution, and tumor tissue sections were stained with H&E or incubated with a monoclonal antibody to adrenocorticotropin (ACTH) (N1531; Dako) or PCNA (PC10; Sigma), and bound primary antibody was detected with the ENVISION/HRP system (Dako). ACTH-stained sections were pretreated in 0.105 M citrate buffer (pH 6.0) at 120°C for 1 min. All counterstaining was performed with 0.5% methyl blue (Sigma) in 0.1 M sodium acetate buffer (pH 4.0).

Quantifications. MHC staining and RNase protection assay results were quantified as described elsewhere (38). For quantification of ACTH staining, the intensities of signals in four fields were measured with the aid of the NIH Image program (version 1.61), and the relative level of signal was determined after the level in tumors from $Rb^{+/-}$ K-$ras^{+/+}$ mice was set to 1.0. For quantification of PCNA staining, the numbers of positive nuclei and total nuclei were counted in four fields. The relative expression ratio was calculated on the basis of the ratio in tumors from $Rb^{+/-}$ K-$ras^{+/+}$ mice, which was set to 1.0.

RNase protection assay. RNase protection assays were performed as described elsewhere (38).

Statistics. Differences in the survival of adult mice and in areas occupied by tumors were analyzed by the log rank test and Fisher's exact test, respectively. A P value of <0.05 was considered to indicate a significant difference.

PCR analysis of tumor DNA. Pituitary tumor regions were marked while in paraffin blocks after observation of corresponding areas in H&E-stained sections and were manually dissected. Subsequently, paraffin blocks were first subjected to a brief heat treatment at 65°C and then suspended in 1× lysis buffer (Applied Biosystems) in the presence of 20 μg of proteinase K (Sigma)/ml at 55°C for 16 h, after which genomic DNA was extracted as described elsewhere (38). PCR was used to determine the genotype for *Rb* and K-*ras* as described previously (15, 16).

MEFs and transcriptional transactivation assays. MEFs were isolated, and MyoD transcriptional transactivation experiments were performed, as described previously (38). pBabe-K-ras^{wt} was constructed by PCR amplification using primers 5′-CGCGGATCCGCCACCATGACTGAATATAAACTTGTGGTAGTT-3′ and 5′-CTGCAGAACCAATGCATTGGTTACATAATTACACACTTTGTCTTTGACTT-3′ with pZIPNeoSV(X)I-EE-K-ras4B (17) as the template, followed by digestion with BamHI and BstXI. The sequence was confirmed after subcloning into pBabe-puro. The plasmid encoding H-Ras^{V12} (pCXN2-H-rasV12 [37]) and those encoding pRb (pSG5L-HA-RB), pRb(661W) (pSG5L-HA-RB; 661W), pRb(Δex4) (pSG5L-HA-RBΔex4), and pRb(Δex22) (pSG5L-HA-RBΔex22) (34) have been described elsewhere. MyoD expression was detected by using a polyclonal antibody (M-318; Santa Cruz Biotechnology).

MyoD infection and BrdU incorporation assay. MEFs were infected with a retrovirus encoding MyoD as described elsewhere (38). Forty-eight hours after infection, cells were incubated in differentiation medium (Dulbecco's modified Eagle medium [DMEM] supplemented with 2% horse serum and 10 μg of insulin [Sigma]/ml) for 72 h. In one experiment, cells were further incubated in differentiation medium in the presence of 10 μM BrdU (Becton Dickinson) for 24 h. In another, cells were subsequently restimulated with 20% fetal bovine serum (FBS) in DMEM containing 10 μM BrdU for 24 h. Cells were fixed and stained with an anti-BrdU antibody (B44; Becton Dickinson) as described previously (38). The percentage of cells incorporating BrdU was determined by scoring at least 300 cells.

Cell cycle analysis. MEFs were maintained in DMEM supplemented with 10% FBS and were harvested with 0.5% trypsin–0.53 mM EDTA. Cells resuspended in PBS were stained with 50 μg of propidium iodide (Molecular Probes)/ml for 30 min in the presence of 0.5 mg of RNase A (Sigma)/ml and were then analyzed by flow cytometry (FACSVantage flow cytometer; Becton Dickinson).

Measurement of K-Ras activity. K-Ras activity was measured as described elsewhere (22). Five hundred micrograms of whole-cell lysate was used to perform each assay, and 50 μg was used for determination of total K-Ras protein by using a c-K-Ras-specific monoclonal antibody (234-4.2; Sigma).

TABLE 1. Timing of lethality in progeny arising from $Rb^{+/-}$ × K-$ras^{+/-}$ crosses[a]

Stage	No. of live (nonviable) embryos recovered[b]					
	$Rb^{+/+}$ K-$ras^{+/+}$	$Rb^{+/+}$ K-$ras^{+/-}$	$Rb^{+/+}$ K-$ras^{-/-}$	$Rb^{-/-}$ K-$ras^{+/+}$	$Rb^{-/-}$ K-$ras^{+/-}$	$Rb^{-/-}$ K-$ras^{-/-}$
E9.5	2	6	2	3	5	3 (8)
E10.5	3	7	3 (1)	3	6	(3)
E11.5	6	12	5 (2)	5	8	(2)
E12.5	4	11	4 (1)	5 (3)	11	(4)
E13.5	7	13	4 (3)	4 (4)	12 (1)	(5)
E14.5	9	17	4 (5)	3 (7)	15 (3)	ND
E15.5	6	10	2 (4)	(5)	7 (4)	ND
E16.5	7	10	1 (5)	(6)	(10)	ND

[a] Embryos with the indicated genotypes were recovered at different embryonic stages and assessed for viability (beating heart).
[b] ND, no data (no embryos were recovered).

RESULTS

Prolonged life spans of *Rb*-deficient embryos lacking a single K-*ras* allele. *Rb*-deficient embryos die at midgestation, displaying a number of developmental abnormalities. Thus, we first tested whether loss of one or both alleles of K-*ras* prolonged the survival of *Rb*-deficient embryos. When $Rb^{+/-}$ K-$ras^{+/-}$ mice were intercrossed, no viable $Rb^{-/-}$ K-$ras^{+/-}$ or $Rb^{-/-}$ K-$ras^{-/-}$ pups were recovered. Embryonic viability was then assessed during a time course of gestation (Table 1). Most *Rb* nullizygous embryos were dead at E14.5 (70%), and no viable embryos were recovered at E15.5 or beyond, in agreement with previous reports (5, 15, 21). K-*ras*-deficient embryos showed a broad window in the timing of their deaths, as previously reported (16, 18). Remarkably, most *Rb*-deficient embryos lacking a single allele of K-*ras* were alive at E14.5 (83%) and E15.5 (64%). Moreover, they displayed a normal appearance, like that of their wild-type littermates (Fig. 1), although the crown-to-rump length, estimated from H&E-stained midsagittal sections, was 11.2% less (at E13.5; $n = 12$) for $Rb^{+/-}$ K-$ras^{+/-}$ embryos than for their wild-type littermates. $Rb^{-/-}$ animals typically showed highly edematous features, leading to increased crown-to-rump length (7.6% at E12.5; $n = 5$) compared to that of wild-type littermates. By contrast, loss of both

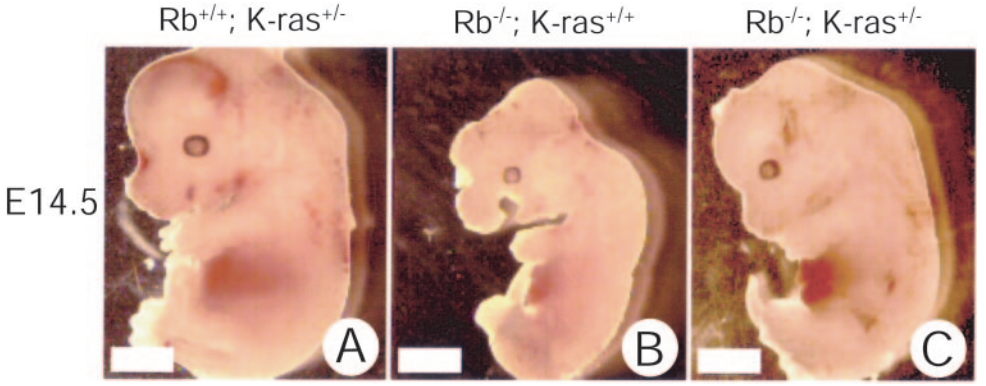

FIG. 1. Effects of heterozygous loss of K-*ras* on the appearance of *Rb*-deficient embryos. Live littermate embryos with the indicated genotypes were recovered at E14.5 and immediately photographed in saline. Bars, 1.0 mm.

alleles of K-*ras* and *Rb* resulted in death as early as E9.5 (Table 1) (data not shown). These results suggest that loss of one but not both alleles of K-*ras* can significantly prolong the survival of the *Rb*-deficient embryo.

Improved skeletal muscle development in *Rb*-deficient embryos following loss of a single K-*ras* allele. Given the results noted above, we asked whether heterozygosity for K-*ras* might reverse some of the developmental abnormalities that characterize *Rb*-deficient embryos. The most prominent cell-autonomous defects resulting from loss of *Rb* are those in skeletal muscle development at midgestation (7, 45, 47). Some of these abnormalities become more pronounced and apparent at late gestational stages. Specifically, embryos lacking *Rb* and *E2f1* (41), *E2f3* (49), or *Id2* (20), or with partial restoration of *Rb* expression (47), or mutant embryos supplied with a wild-type placenta (7, 45), all of which live longer than *Rb*-deficient embryos, show similar defects in muscle development. Abnormalities include reduced myotube length, fiber density, and expression of late markers of differentiation, as well as evidence of ectopic S-phase entry and cell death. We determined whether loss of a single allele of K-*ras* affected these *Rb*-dependent phenotypes.

Axial muscles from live $Rb^{+/+}$ K-$ras^{+/-}$, $Rb^{-/-}$ K-$ras^{+/+}$, and $Rb^{-/-}$ K-$ras^{+/-}$ E14.5 littermates were compared. H&E staining of *Rb*-deficient muscle sections revealed a conspicuous reduction in muscle fiber density compared to $Rb^{+/+}$ K-$ras^{+/-}$ tissue (Fig. 2A to C). This defect was most pronounced in sections immunostained with an antibody to MHC (Fig. 2D and E). MHC-stained sections also showed reductions in the length and thickness of individual myotubes. In contrast, $Rb^{-/-}$ K-$ras^{+/-}$ axial muscle showed near-normal fiber density (Fig. 2F and J) as well as thickness and length of myotubes (Fig. 2F and K). These features were noted despite evidence of continuing DNA replication (Fig. 2C and L), shown previously to be indicated by abnormally large nuclei (47), and cells undergoing apoptosis (Fig. 2G to I and M). Together, these results suggest that loss of one K-*ras* allele prevents, although incompletely, the reduction in muscle fiber density and irregular myotube formation that characterize *Rb*-deficient skeletal muscle, despite having no impact on ectopic DNA synthesis or cell death.

At the molecular level, *Rb*-deficient muscle is characterized by a failure to induce certain markers of differentiation, e.g., muscle creatine kinase (MCK) (47), which has been linked to a defect in MyoD transcriptional activity (27). Analysis of transcript levels revealed that loss of a single K-*ras* allele resulted in restoration in *MCK* expression in *Rb*-deficient skeletal muscle (Fig. 2N). We also assessed the influence of K-*ras* heterozygosity in *Rb*-deficient cells on MyoD function. To this end, $Rb^{+/+}$ K-$ras^{+/+}$, $Rb^{+/+}$ K-$ras^{+/-}$, $Rb^{-/-}$ K-$ras^{+/+}$, and $Rb^{-/-}$ K-$ras^{+/-}$ MEFs were generated. MEFs were transfected with a plasmid encoding MyoD and an MCK promoter reporter and were subsequently cultured under conditions known to induce myogenic differentiation. The activity of MyoD was significantly lower in $Rb^{-/-}$ K-$ras^{+/+}$ myoblasts than in those expressing wild-type *Rb* (Fig. 3A). In contrast, $Rb^{-/-}$ K-$ras^{+/-}$ myoblasts displayed normal levels of MyoD activity. To rule out the possibility that events secondary to the loss of *Rb* or K-*ras* might account for the results described above, a number of experiments were performed. Reintroduction of *Rb* into *Rb*-deficient myoblasts restored the activity of MyoD, and oncogenic *ras* could overcome this effect (Fig. 3B), observations that are consistent with the notion that deregulated Ras signaling following loss of *Rb* leads to inhibition of MyoD. Further, ectopic expression of either wild-type K-*ras* or oncogenic H-*ras* in $Rb^{-/-}$ K-$ras^{+/-}$ myoblasts leads to inhibition of MyoD transcriptional activity (Fig. 3B). By contrast, introduction of K-*ras* into $Rb^{+/+}$ K-$ras^{+/-}$ myoblasts has no effect on MyoD activity (Fig. 3B). This suggests that a certain level of endogenous K-Ras activity is required for the negative effect of *Rb* loss on MyoD activity to be manifest and that the specific loss of K-*ras* in the context of *Rb* nullizygosity is responsible for the restoration of MyoD activity in $Rb^{-/-}$ K-$ras^{+/-}$ myoblasts. Together, these in vivo and in vitro analyses suggest that loss of a single K-*ras* allele can reverse the defect in MyoD function resulting from deficiency in *Rb*.

Though the ability of pRb to influence cell cycle progression and MyoD function are genetically separable (34), it is formally possible that in the absence of *Rb*, heterozygosity for K-*ras* influences the ability of myoblasts to withdraw from the cell cycle, which in turn affects MyoD activity. To explore this possibility, the abilities of $Rb^{+/+}$ K-$ras^{+/-}$, *Rb*-deficient, and $Rb^{-/-}$ K-$ras^{+/-}$ myoblasts to withdraw from the cell cycle during myogenic differentiation were compared. MEFs were infected with a retrovirus encoding MyoD and subsequently cultured under conditions known to induce differentiation, and

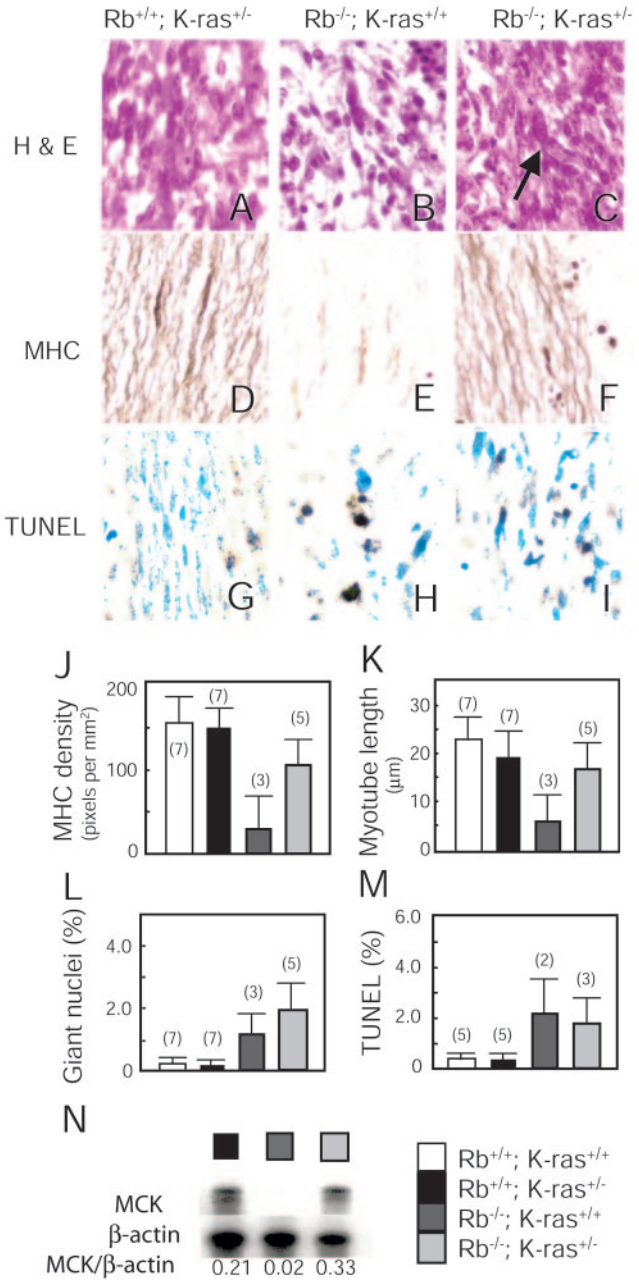

FIG. 2. Effects of heterozygous loss of K-*ras* on skeletal muscle development in E14.5 *Rb*-deficient embryos. (A to F) Longitudinal sections through the fibers of thoracic somite-associated skeletal muscles from sagittal sections of live E14.5 embryos derived from the same litter with the indicated genotypes were stained with H&E (A to C) or immunostained with an antibody to MHC (D to F). A large nucleus (arrow) in myotubes is indicated in panel C. Magnification, ×40. (G to I) Apoptosis (TUNEL) observed in myoblasts of thoracic skeletal muscles of live E14.5 embryos of the indicated genotypes. Magnification, ×40. (J) Density of MHC staining in myotubes. Ten myotubes per embryo were analyzed; average densities of the MHC signal ± standard errors are shown. Numbers of embryos analyzed are given in parentheses. (K) The lengths of myotubes immunostained with an antibody to MHC were quantified. Longitudinal sections of thoracic skeletal muscles from live E14.5 embryos were analyzed by microscopic observation. Twenty myotubes per embryo were measured; average lengths ± standard errors are presented. Numbers of embryos analyzed are given in parentheses. (L) One hundred myotubes in the thoracic skeletal muscle were analyzed for the presence of giant nuclei following staining with H&E. Average percentages ± standard errors are presented. Numbers of embryos analyzed are given in parentheses. (M) The level of apoptosis was quantified by counting the frequency of TUNEL-positive cells per 300 nuclei analyzed in the thoracic muscle. Average percentages ± standard errors are presented. Numbers of embryos analyzed are given in parentheses. (N) Expression of *MCK* in live E14.5 littermates determined by RNase protection assays with RNAs derived from carcasses. Ratios of *MCK* to β-*actin* expression are given below the autoradiograph.

the incorporation of BrdU was measured as an indication of ongoing DNA synthesis. Low levels of BrdU incorporation were noted in $Rb^{+/+}$ K-$ras^{+/-}$ as well as in $Rb^{-/-}$ and $Rb^{-/-}$ K-$ras^{+/-}$ myoblasts (Fig. 3C), indicating that K-*ras* heterozygosity did not influence the ability of $Rb^{-/-}$ myoblasts to withdraw from the cell cycle during differentiation. However, upon restimulation of these differentiated myoblasts, both $Rb^{-/-}$ and $Rb^{-/-}$ K-$ras^{+/-}$ myoblasts, unlike those harboring wild-type *Rb*, showed higher levels of BrdU incorporation (Fig. 3C). These results are in keeping with the previous demonstration that *Rb*-deficient myoblasts fail to maintain a terminal cell cycle arrest (27), and they indicate that K-*ras* heterozygosity does not rescue this defect. Further, we determined whether two pRb mutants, 661W and Δex4, previously shown to be deficient in bringing about G_1 arrest but to retain the ability to positively affect MyoD activity in an osteosarcoma cell line (34), could restore MyoD activity in our system. These mutants, but not a pRb-null mutant (Δex22), were capable of potentiating MyoD activity in *Rb*-deficient myoblasts to a level comparable to that observed with the wild-type protein (Fig. 3D). Further, when analyzed in $Rb^{-/-}$ K-$ras^{+/-}$ myoblasts, pRb(661W) and pRb(Δex4) did not further activate MyoD (Fig. 3D), reinforcing the notion that restoration of appropriate cell cycle regulation is not required in a significant way to restore MyoD function in $Rb^{-/-}$ myoblasts.

To analyze the cell cycle issue further, asynchronous populations of MEFs were studied. In agreement with previous observations, *Rb*-deficient MEFs displayed higher percentages of cells in S and G_2/M than wild-type MEFs (Fig. 3E). $Rb^{-/-}$ K-$ras^{+/-}$ MEFs showed a cell cycle distribution similar to that of *Rb*-deficient cells (Fig. 3E), suggesting that loss of a single K-*ras* allele does not influence the distribution of cells in each of the cell cycle phases. These findings are consistent with the previous demonstration that *Rb*-deficient cells, unlike wild-type cells, fail to arrest in G_1 following a block to Ras function (23, 26, 30). In addition, we confirmed that heterozygosity for K-*ras* does reduce the level of Ras activity for this isoform by approximately one-half (Fig. 3F). Together with the observations noted above, these findings suggest that loss of a single K-*ras* allele in *Rb*-deficient cells has a more profound impact on the ability of these cells to differentiate than on their cell cycle distribution.

K-*ras* heterozygosity does not affect the deregulated proliferation that characterizes *Rb*-deficient embryos. *Rb*-deficient embryos are characterized by deregulated proliferation and apoptosis in the CNS and peripheral nervous system (PNS) and the developing lens (5, 15, 21), which occur in a cell-autonomous or non-cell-autonomous manner (7, 25, 45). To determine whether loss of one K-*ras* allele affected these *Rb*-dependent phenotypes, BrdU was injected into pregnant fe-

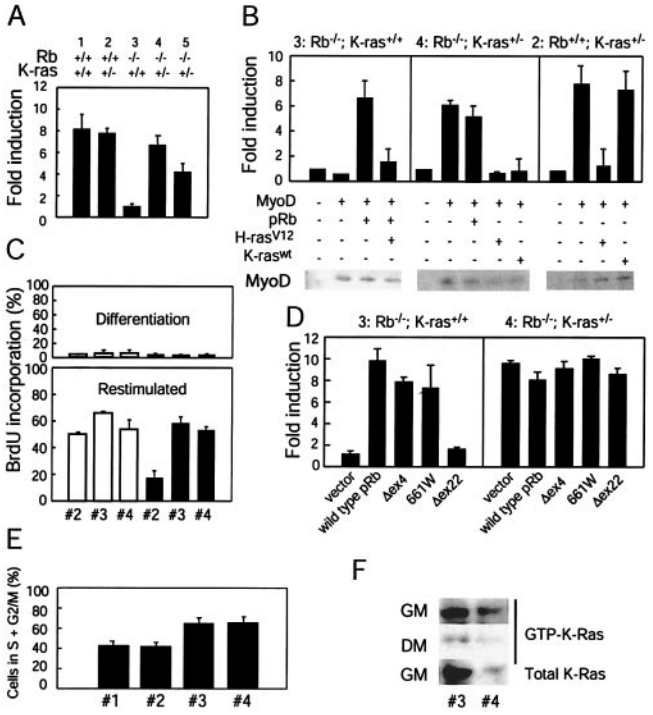

FIG. 3. Effects of K-*ras* heterozygosity on MyoD transcriptional activity in *Rb*-deficient myoblasts. (A) MEFs of the indicated genotypes were transfected with an MCK promoter reporter construct (MCK-luc; 0.25 μg), pCSA-MyoD (1.25 μg), and pCMV-β-gal (0.25 μg). Twenty-four hours later, the cells were placed in differentiation medium for 48 h. Luciferase and β-galactosidase activities were determined, and normalized fold activations were calculated relative to the corrected luciferase activity in the absence of MyoD. Results are means ± standard errors for three independent experiments performed in triplicate. Numbers above the bar graph represent the particular MEFs used; groups 1 and 5 are derived from matched littermates, as are groups 2, 3, and 4. (B) MEFs 3, 4, and 2 were transfected as described for panel A. Plasmids encoding pRb (0.25 μg), H-ras^{V12} (0.5 μg), and K-ras^{wt} (0.5 μg) were included in the transfections as indicated. Fold activations were calculated relative to the corrected luciferase activity in the absence of MyoD. Results are means ± standard errors for three independent experiments performed in triplicate. Immunoblots for ectopically expressed MyoD are shown. (C) MEFs 2, 3, and 4 (designations as described for panel A) were infected with a retrovirus encoding MyoD (filled bars) or empty vector (open bars) and cultured under differentiation conditions for 72 h. Subsequently, cells were either further cultured in differentiation medium or restimulated with 20% FBS in the presence of BrdU for 24 h. Percentages of cells incorporating BrdU under differentiation conditions (upper panel) and following restimulation (lower panel) were determined. Results are means ± standard errors for two independent experiments. (D) MEFs 3 and 4 were transfected as described for panel A. A plasmid (0.25 μg) encoding pRb, pRb(661W), pRb(Δex4), or pRb(Δex22), or a vector control, was included in the transfection as indicated. Cells were treated as described for panel A, and fold activations were calculated relative to the corrected luciferase activity in the absence of MyoD. Results are means ± standard errors from three independent experiments performed in duplicate. (E) The cell cycle distribution of asynchronous cultures of MEFs 1, 2, 3, and 4 (designations as described for panel A) was determined by fluorescence-activated cell sorting. Results are means ± standard errors for percentages of cells in S and G_2/M from four independent experiments. (F) MEFs 3 and 4 (designations as described for panel A) were cultured in 2% horse serum (differentiation medium [DM]) for 72 h. At this time, the level of activated, GTP-bound K-Ras was determined (middle panel). Alternatively, cells cultured in the presence of horse serum (low levels of mitogens) were restimulated with 20% fetal bovine serum (growth medium [GM]) for 6 h; at this time, the level of active K-Ras was determined (top panel). Whole-cell lysates were analyzed for total K-Ras protein levels (bottom panel). Results are representative of three independent experiments.

males at day 13.5 of term, and immunological detection of incorporated BrdU was used as a measure of DNA synthesis. BrdU-positive cells were readily apparent in the intermediate zone of the hindbrain (CNS) in *Rb*-deficient but not wild-type embryos (Fig. 4A and B). Analysis of $Rb^{-/-}$ K-$ras^{+/-}$ embryos also revealed ectopic DNA synthesis in this tissue (Fig. 4C). Similar findings were made upon inspection of the dorsal root ganglion of the PNS and the fiber cell compartment of the lens (Fig. 4G). TUNEL staining was used to detect apoptosis. $Rb^{-/-}$ K-$ras^{+/-}$ embryos, like *Rb*-deficient embryos, showed elevated levels of apoptosis in the cortical region around the fourth ventricle of the brain (CNS) (Fig. 4D to F), in the PNS, and in the lens compared to those for wild-type embryos (Fig. 4H). These results suggest that the ectopic proliferation and cell death observed in *Rb*-deficient embryos are not affected by the loss of a single K-*ras* allele.

Heterozygosity for K-*ras* affects the differentiation status of pituitary tumors resulting from loss of *Rb*. $Rb^{+/-}$ mice are tumor prone, resulting in their shorter life span. Given the results noted above indicating that heterozygosity for *K-ras* rescues a unique subset of developmental defects associated with *Rb* nullizygosity, we determined whether loss of a single K-*ras* allele affects the survival of *Rb* heterozygotes.

To determine whether loss of a single K-*ras* allele affects the viability of *Rb* heterozygotes, a cohort of $Rb^{+/-}$ K-$ras^{+/+}$ and $Rb^{+/-}$ K-$ras^{+/-}$ mice was observed for 600 days after birth. Loss of a single K-*ras* allele was found to significantly prolong the survival of *Rb* heterozygotes ($P = 0.0054$ by the log rank test) (Fig. 5). The mean age at death of *Rb* heterozygotes was 270 days (range, 210 to 381 days; standard deviation, ±24 days). In contrast, the mean age at death for $Rb^{+/-}$ K-$ras^{+/-}$ mice was 381 days (range, 241 to 598 days; standard deviation, ±96 days), representing a 41% extension in the life span with loss of a single K-*ras* allele. Several $Rb^{+/-}$ K-$ras^{+/-}$ mice (6%) survived beyond 598 days, while no $Rb^{+/-}$ K-$ras^{+/+}$ animals lived past 381 days. The survival curve for $Rb^{+/+}$ K-$ras^{+/-}$ animals was similar to that of wild-type mice, with more than 90% living beyond 600 days (data not shown). These observations suggest that heterozygosity for K-*ras* can extend the life spans of $Rb^{+/-}$ mice.

Rb heterozygotes develop pituitary adenocarcinomas of the intermediate lobe, resulting in compression of the brain, and medullary (C-cell) thyroid adenomas at high frequencies; the former are responsible for their shorter survival. To examine if loss of a single K-*ras* allele affects either the incidence or the size of pituitary tumors, we observed the intracranial structures in sick mice after sacrifice and perfusion with a fixative. Frequencies of appearance of macroscopically detectable pituitary tumors were similar in $Rb^{+/-}$ K-$ras^{+/+}$ (96%) and $Rb^{+/-}$ K-$ras^{+/-}$ (93%) mice, suggesting that loss of a single K-*ras* allele had no effect on the penetrance of pituitary tumor formation in *Rb* heterozygotes.

$Rb^{+/-}$ K-$ras^{+/+}$ and $Rb^{+/-}$ K-$ras^{+/-}$ mice developed tumors of the melanotrophic cells that occupy the intermediate lobe of the pituitary gland. Histological analysis revealed that, at the

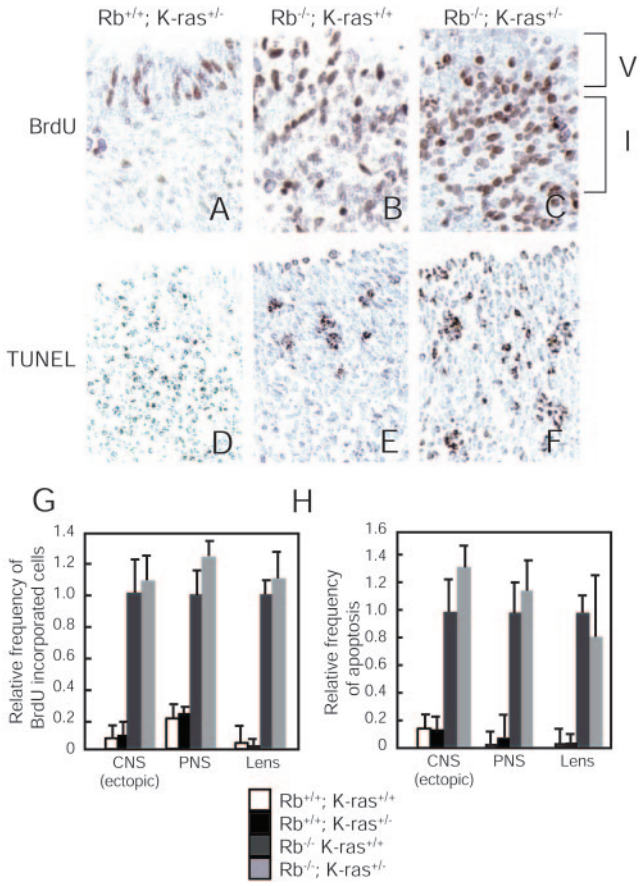

FIG. 4. Effects of heterozygous K-*ras* loss on ectopic S-phase entry and cell death. (A-C) Transverse sections of the ventricular (V) and intermediate (I) zones of the hindbrain in the CNS from E13.5 embryos of the indicated genotypes were stained for cells in S phase (BrdU). Magnification, ×20. (D-F) Midsagittal sections of the cortical region around the fourth ventricle from E13.5 embryos of the indicated genotypes were stained for apoptotic cells (TUNEL). Magnification, ×20. (G) The level of ectopic S-phase entry was quantified by counting the frequency of BrdU-positive cells per unit area in tissue sections of the intermediate zone of the hindbrain (CNS [ectopic]), dorsal root ganglia (PNS), and fiber compartment of the lens (Lens). Total cell numbers were determined by counting cells counterstained with methyl blue. $Rb^{-/-}$ samples were set to 1.0, and the relative ratios of BrdU-positive cells are displayed. Values are means ± standard errors for two to four embryos. (H) The level of apoptosis was quantified by counting the frequency of TUNEL-positive cells per unit area of tissues: the cortical region around the fourth ventricle of the CNS, the dorsal root ganglia of the PNS, and the fiber compartment of the lens. Total cell numbers were determined by counting cells counterstained with methyl blue. $Rb^{-/-}$ samples were set to 1.0, and the relative ratios of TUNEL-positive cells are displayed. Values are means ± standard errors for two to four embryos.

time of death, tumors arising in $Rb^{+/-}$ K-$ras^{+/-}$ mice tended to be larger than those in $Rb^{+/-}$ K-$ras^{+/+}$ animals (data not shown), raising the possibility that the prolonged survival of $Rb^{+/-}$ K-$ras^{+/-}$ mice may be a result of their developing less-aggressive pituitary tumors.

To investigate this issue further, mice were sacrificed at a specific time and then compared. Analysis of animals at 280 days, representing the mean survival of *Rb* heterozygotes, revealed that the areas of tumors arising in $Rb^{+/-}$ K-$ras^{+/-}$ mice were 1.8-fold smaller than those in $Rb^{+/-}$ K-$ras^{+/+}$ animals (Table 2), suggesting that pituitary tumors grow more slowly in mice lacking a single K-*ras* allele. Tumors in $Rb^{+/-}$ K-$ras^{+/-}$ mice analyzed at the age of 360 days (mean survival of $Rb^{+/-}$ K-$ras^{+/-}$ mice) were similar or even larger than those in $Rb^{+/-}$ K-$ras^{+/+}$ mice at the age of 280 days (Table 2), suggesting that for the same tumor volume in the two genotypes, those arising in $Rb^{+/-}$ K-$ras^{+/-}$ mice might cause less intracranial pressure due to adaptation over time. Further, pituitary tumors arising in $Rb^{+/-}$ K-$ras^{+/+}$ mice displayed signs of local invasion and were poorly encapsulated; these features were significantly less pronounced in tumors occurring in $Rb^{+/-}$ K-$ras^{+/-}$ mice (Fig. 6A, B, and G).

Morphological studies of pituitary tumors were performed, restricting the analysis to the window of time when 80 to 20% of the mice were still alive for the respective genotypes. The majority of tumors arising in $Rb^{+/-}$ K-$ras^{+/+}$ mice showed a poorly differentiated, diffuse pattern of growth (Fig. 6C and H). In striking contrast, most tumors analyzed in $Rb^{+/-}$ K-$ras^{+/-}$ animals displayed a well-differentiated sinusoidal pattern of growth (Fig. 6D and H). Indeed, a sinusoidal morphology is one of the features used to distinguish pituitary adenomas from pituitary adenocarcinomas (1). This suggests that loss of a single K-*ras* allele results in the formation of less-aggressive pituitary tumors owing to their more-differentiated phenotype.

To explore the differentiation status of the pituitary tumors further, ACTH expression was studied. Secretion of ACTH is often associated with melanotrophic tumors of the intermediate lobe (1), and it has been reported that there is an inverse correlation between ACTH levels and the aggressiveness of pituitary tumors (43). Analysis of several mice at the approximate median survival for the cohort revealed that pituitary tumors arising in $Rb^{+/-}$ K-$ras^{+/-}$ mice express significantly higher levels of ACTH than those in $Rb^{+/-}$ K-$ras^{+/+}$ animals (Fig. 6I, J, and M), consistent with the morphological studies

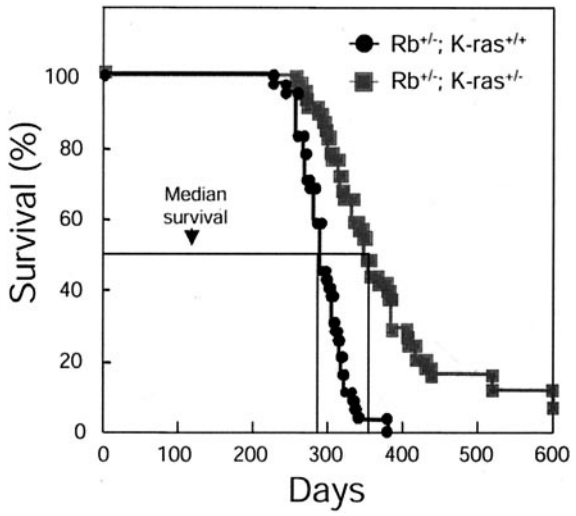

FIG. 5. Effects of K-*ras* heterozygosity on the survival of $Rb^{+/-}$ mice. Progeny arising from $Rb^{+/-}$ × K-$ras^{+/-}$ intercrosses were aged together. Shown are survival curves for $Rb^{+/-}$ K-$ras^{+/+}$ (n = 44) and $Rb^{+/-}$ K-$ras^{+/-}$ (n = 48) mice. Percent survival represents the percentage of the initial starting population surviving at a given age (in days) for the indicated genotype. Median survival is indicated.

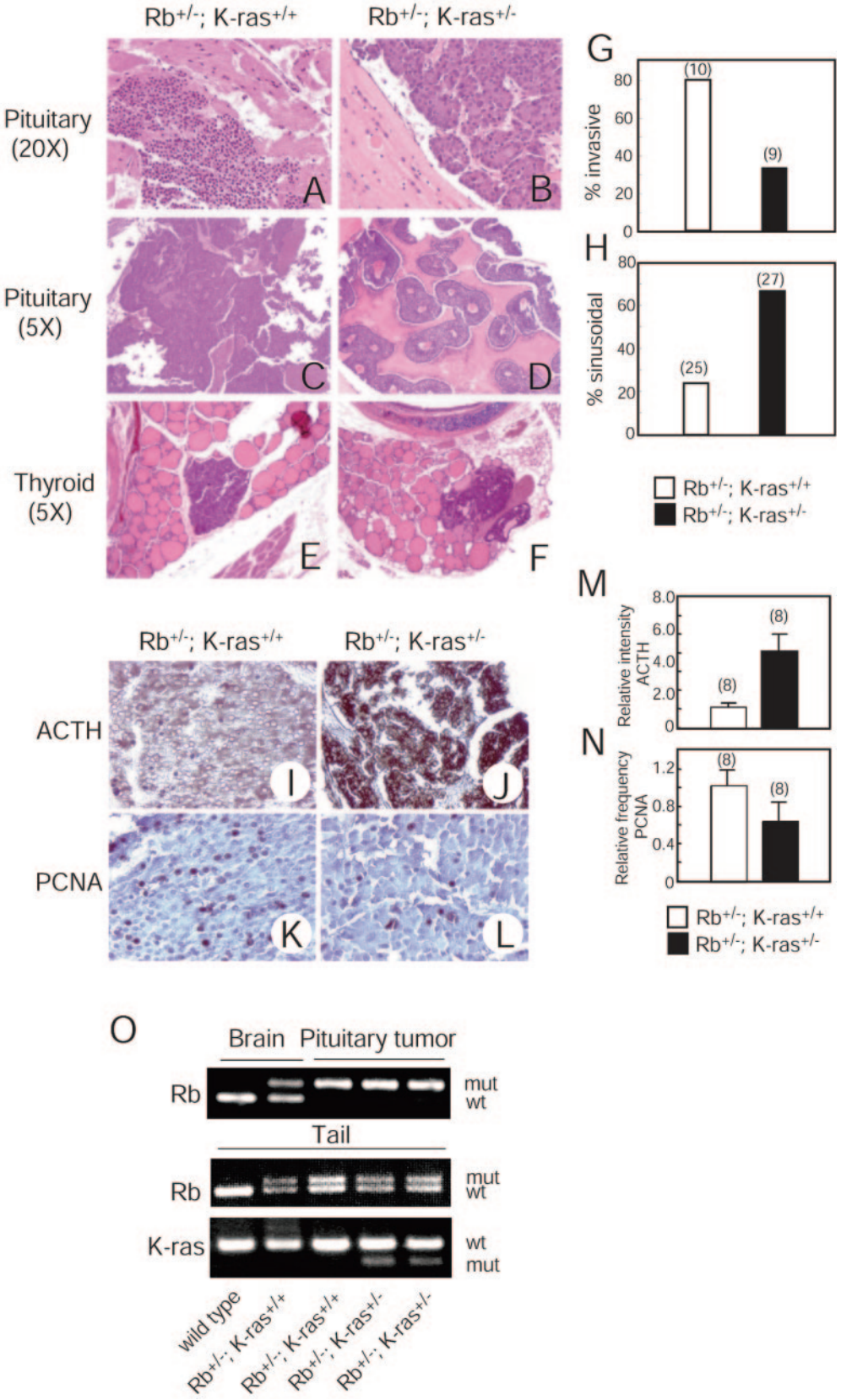

FIG. 6. Effects of K-*ras* heterozygosity on characteristics of tumors arising in $Rb^{+/-}$ mice. (A-D) H&E-stained sections of pituitary adenocarcinomas from mice of the indicated genotypes. Magnifications, ×18 (A and B) and ×4.5 (C and D). Original magnifications are given in parentheses. (E and F) H&E-stained sections of C-cell adenomas from mice of the indicated genotypes. Magnification, ×4.5. Original magnification is given in parentheses. (G) Frequency of appearance of invasive tumors. Genotypes and numbers of mice analyzed are given. (H) Frequency

TABLE 2. Comparison of pituitary tumor sizes[a]

Measurement	$Rb^{+/-}$ K-$ras^{+/+}$ mice at 280 days ($n = 10$)	$Rb^{+/-}$ K-$ras^{+/-}$ mice at 280 days ($n = 8$)	$Rb^{+/-}$ K-$ras^{+/-}$ mice at 360 days ($n = 6$)
Mean area (mm^2) ± SD	38.9[b] ± 9.6	21.6[b] ± 11.2	53.6 ± 12.0
Range (minimum to maximum)	12.0–51.2	11.2–44.8	19.2–61.2

[a] Pituitary tumors were observed in mice with the indicated genotypes and ages. Tumor areas were determined under microscopy at the median section of tumors stained with H&E by measuring the longest diameter and its longest perpendicular line.
[b] $P = 0.029$.

described above. We also analyzed the growth fraction of the tumors by staining the same sections used in the ACTH studies for PCNA. Per unit area, pituitary tumors arising in $Rb^{+/-}$ K-$ras^{+/-}$ mice showed a 30% reduction in the frequency of PCNA-positive cells compared to those in $Rb^{+/-}$ K-$ras^{+/+}$ animals (Fig. 6K, L, and N). Loss of the remaining wild-type *Rb* allele was observed in pituitary tumors from both $Rb^{+/-}$ K-$ras^{+/+}$ and $Rb^{+/-}$ K-$ras^{+/-}$ mice, suggesting that K-*ras* heterozygosity does not influence this genetic event (Fig. 6O). Together these observations suggest that the reduced volume of the tumors arising in $Rb^{+/-}$ K-$ras^{+/-}$ mice is due to their more-differentiated characteristics and somewhat lower proliferative activity rather than to delayed tumor onset.

C-cell tumors resulting from loss of *Rb* cannot be detected macroscopically. Histological analysis of multiple sections revealed that 100% of the $Rb^{+/-}$ K-$ras^{+/+}$ mice developed C-cell adenomas ($n = 26$). Similar findings were noted for $Rb^{+/-}$ K-$ras^{+/-}$ mice ($n = 26$). $Rb^{+/-}$ K-$ras^{+/+}$ and $Rb^{+/-}$ K-$ras^{+/-}$ mice sacrificed at 280 days after birth showed the presence of histologically similar tumors (Fig. 6E and F). These data suggest that, in contrast to pituitary adenocarcinomas, loss of a K-*ras* allele does not influence the initiation or progression of medullary thyroid adenomas resulting from loss of *Rb*.

DISCUSSION

A block to differentiation is thought to contribute to tumor formation. However, there is little understanding of the genetic pathways that contribute to tumorigenesis by disrupting the processes of differentiation (39). Part of this difficulty stems from the observation that aberrant alterations in cell cycle control can hinder the normal execution of various differentiation programs. This can complicate efforts to dissect the relative contributions of specific pathways governing cell cycle progression and differentiation to tumorigenesis. pRb is a case in point, as it is involved in both processes. Genetic alterations affecting components of the pRb pathway (*Rb*, *cyclin D*, *cdk4*, *p16*) leading to deregulation of E2F activity are thought to provide tumors with a selective advantage by increasing their proliferative potential. It is likewise well established that pRb can also positively regulate differentiation through mechanisms distinct from its regulation of E2F and proliferation. And in this study we provide genetic evidence that the ability of pRb to promote differentiation is linked to its tumor suppressor function.

Several defects characterize *Rb*-deficient embryos, most notably a failure in fetal liver erythropoiesis, ectopic proliferation and apoptosis of the central and peripheral nervous systems and lens, and aberrant differentiation of skeletal muscle. Recently, it has been demonstrated that the origin of the defect in erythropoiesis and ectopic apoptosis in the central nervous system is the *Rb*-deficient placenta and not the embryo proper, while the other abnormalities noted above still persist when *Rb*-deficient embryos are supplied with a wild-type placenta (7, 45). Our finding that loss of a single K-*ras* allele can extend the life spans of *Rb*-deficient embryos suggests that fetal liver erythropoiesis is improved in these animals. Preliminary studies indicate that $Rb^{+/-}$ K-$ras^{+/-}$ embryos do display an increased hematocrit compared to that of *Rb* heterozygotes, likely reflecting at least a partial rescue of erythropoiesis (C. Takahashi, M. Socolovsky, and M. E. Ewen, unpublished data). Further, heterozygosity for K-*ras* rescues many of the skeletal muscle defects that characterize *Rb*-deficient embryos. By contrast, we find no effect of K-*ras* heterozygosity on the ectopic proliferation and apoptosis observed in the CNS, PNS, and lens resulting from *Rb* deficiency. Thus, loss of K-*ras* appears to affect a unique subset of developmental defects that characterize *Rb*-deficient embryos.

The differentiation function of pRb has been best characterized for myogenesis; the requirement for *Rb* during skeletal muscle differentiation has been documented both in vivo and in vitro. Cell culture studies indicate that pRb controls myogenesis in an E2F-independent manner (34). In agreement with this observation, *Rb E2f* compound embryos, while living longer than *Rb*-deficient embryos, continue to display abnormalities in muscle differentiation (41, 49). Our findings suggest that the genetic interaction between *Rb* and *ras* has a significant role in skeletal muscle development. Loss of a single K-*ras* allele rescued many of the defects that characterize *Rb*-deficient skeletal muscle, including fiber density and myotube length. Importantly, expression of MCK, a late marker of muscle differentiation and a transcriptional target of MyoD, was also rescued. Consistent with this observation made in vivo,

of appearance of sinusoidal (versus diffuse) pattern of growth. Genotypes and numbers of mice analyzed are given. (I and J) Anti-ACTH immunostaining of pituitary tumors arising in mice of the indicated genotypes. Magnification, ×18. (K and L) Anti-PCNA immunostaining of pituitary tumors arising in mice of the indicated genotypes. Magnification, ×36. (M) Quantification of ACTH immunostaining. Genotypes and numbers of mice analyzed are given. Bars represent means ± standard errors. (N) Quantification of PCNA immunostaining. Genotypes and numbers of mice analyzed are given. Bars represent means ± standard errors. (O) Genotyping of *Rb* and K-*ras* in normal brain tissue, pituitary tumors, and tails from mice of the indicated genotypes by PCR. The weak band for the wild-type *Rb* allele that appeared in one of the pituitary tumors is likely derived from nontumor cells residing in tumors. wt, wild type; mut, mutant.

heterozygosity for K-*ras* restored MyoD transcriptional activity in myoblasts lacking *Rb*, in the apparent absence of an influence on the cell cycle. Previously, similar observations were made in an analysis of $Rb^{-/-}$ N-$ras^{-/-}$ embryos and myoblasts (38), suggesting that a reduced level of total *ras* is required in order to observe an amelioration of defects brought about by *Rb* deficiency. In contrast to the observed effects on differentiation and MyoD function, loss of a single K-*ras* allele did not suppress ectopic proliferation in developing *Rb*-deficient skeletal muscle. Thus, in a given tissue, skeletal muscle, pRb appears to affect proliferation and differentiation through distinct mechanisms.

Understanding how tumor suppressors such as *Rb* affect processes involved in tumorigenesis is a goal of cancer research. The contribution of the proliferation function of *Rb* to tumor suppression has been established through analysis of *Rb E2f* compound mutant mice (see the introduction). By contrast, no role in tumor suppression has been found for *Rb*'s function in promoting differentiation. However, genetic analysis of *Rb* suggests the possibility that the positive effect of *Rb* on differentiation does contribute to its tumor suppression function. In classical familial retinoblastoma, bilateral tumors are noted in more than 90% of affected individuals. By contrast, *Rb* mutations have been identified where carriers show no signs of disease, develop unilateral retinoblastoma, or suffer benign retinomas (8, 19, 24, 29), suggesting that the protein products encoded by these partially penetrant alleles do possess tumor suppressor activity. Characterization of these pRb mutants in vitro indicates that they fail to interact with E2F (19, 34, 42) yet maintain the ability to promote differentiation (34) and restore the aberrantly high levels of Ras activity observed in *Rb*-deficient cells to normal levels (22). Together, these studies have raised the possibility that *Rb* might function together with *ras* to affect tumor suppression by influencing differentiation.

To test this hypothesis and to extend the observations described above to an in vivo setting, we asked whether loss of a *ras* allele, which should theoretically lower the total level of Ras activity, might affect tumor development in *Rb* heterozygotes. Our studies reveal that this is the case. Loss of a single K-*ras* allele resulted in less-aggressive pituitary tumors and correspondingly increased the life spans of *Rb* heterozygous mice. *Rb* K-*ras* heterozygotes developed smaller pituitary tumors than their age-matched $Rb^{+/-}$ littermates. Importantly, and in consonance with our embryological studies, histological and molecular analyses revealed that loss of a K-*ras* allele resulted in more-differentiated tumors. The modest reduction in the growth fraction of these tumors is likely secondary to their more-differentiated phenotype. These findings are in contrast to those obtained in the analysis of *Rb* heterozygotes lacking *E2f1* or *E2f3*, where it was found that while the sizes of the pituitary tumors were reduced, the tumors were histologically indistinguishable from those arising in $Rb^{+/-}$ animals (46, 48), suggesting that downstream effectors of *Rb* in the control of proliferation do not influence the differentiation status of pituitary tumors resulting from *Rb* loss. Together these observations suggest that loss of *Rb* contributes to pituitary tumorigenesis by affecting differentiation (through K-*ras*) and proliferation (through *E2f*). Consistent with this interpretation, treatment of pituitary tumors arising in $Rb^{+/-}$ mice with an adenovirus expressing wild-type pRb prolonged their survival, and this correlated with a decrease in proliferation and a more-differentiated phenotype (32).

Our analysis of C-cell tumors revealed no effect of K-*ras* deficiency, suggesting that the signaling output from the genetic interaction between *Rb* and K-*ras* influencing the differentiation status during tumor development is cell type specific. Thus far, our embryological studies identify MyoD as a key molecular target of the antagonism between *Rb* and K-*ras* signaling during skeletal muscle development. Only when we identify the repertoire of the effectors of *Rb*/K-*ras* signaling will we understand the tissue-specific nature of the genetic interaction between *Rb* and K-*ras*.

Virtually all studies linking *ras* proto-oncogenes to tumorigenesis pertain to the oncogenic constitutively active forms. By contrast, the work presented here identifies wild-type K-*ras* as a participant in pituitary tumor progression following loss of *Rb*. Thus, there is the possibility that, as a function of the particular genetic lesions driving tumorigenesis and perhaps the tissue type, wild-type *ras* may contribute materially to the malignant behavior of certain cancers. Current strategies that target oncogenic Ras in human tumors (e.g., farnesyltransferase inhibitors) do not distinguish between the mutant constitutively active and wild-type forms. This suggests that such therapeutic strategies may be applied in the context of cancers that harbor wild-type Ras.

ACKNOWLEDGMENTS

We express special thanks to K. Y. Lee, M. Noda, C. McMahon, J. Lamb, D. Livingston, A. Lassar, G. Dranoff, S. Lux, P. Sicinski, M. Ciemerych, W. Kaelin, J. DeCaprio, K. Tsai, R. Takahashi, and T. Arai for help, advice, and encouragement. We thank T. Jacks for kindly providing *Rb* and K-*ras* mutant mice, Y. Itokazu for FACS analysis, T. Kawai and Z. Lee for technical help, J. Jackson, A. Lassar, W. Sellers, J. Miyazaki, and W. Wright for plasmids, and J. Lamb, C. McMahon, W. Sellers, and J. Lee for critical review of the manuscript.

This work was supported by National Institutes of Health grants R01CA65842 (to M.E.E.) and P01CA89021 (to M.L.) and by a Massachusetts Prostate Cancer Research Grant and a grant from the Japanese Ministry of Education and Science to C.T. C.T. was supported in part by the NCI-JFCR Scientist Exchange Program. During this work M.E.E. was a Leukemia and Lymphoma Society Scholar.

REFERENCES

1. **Capen, C. C., E. Karbe, U. Deschl, C. George, P.-G. Germann, C. Gopinath, J. F. Hardisty, J. Kanno, W. Kaufmann, G. Krinke, K. Kuttler, B. Kulwich, C. Landes, B. Lenz, L. Longeart, I. Paulson, E. Sander, and K. Tuch.** 2001. Endocrine system, p. 269–322. *In* U. Mohr (ed.), International classification of rodent tumors: the mouse. Springer-Verlag, Berlin, Germany.
2. **Charles, A., X. Tang, E. Crouch, J. S. Brody, and Z. X. Xiao.** 2001. Retinoblastoma protein complexes with C/EBP proteins and activates C/EBP-mediated transcription. J. Cell. Biochem. **83:**414–425.
3. **Chen, P.-L., D. J. Riley, Y. Chen, and W.-H. Lee.** 1996. Retinoblastoma protein positively regulates terminal adipocyte differentiation through direct interaction with C/EBPs. Genes Dev. **10:**2794–2804.
4. **Chen, P.-L., D. J. Riley, S. Chen-Kiang, and W.-H. Lee.** 1996. Retinoblastoma protein directly interacts with and activates the transcription factor NF-IL6. Proc. Natl. Acad. Sci. USA **93:**465–469.
5. **Clarke, A. R., E. R. Maandag, M. van Roon, N. M. T. van der Lugt, M. van der Valk, M. L. Hooper, A. Berns, and H. te Riele.** 1992. Requirement for a functional *Rb-1* gene in murine development. Nature **359:**328–330.
6. **Classon, M., B. K. Kennedy, R. Mulloy, and E. Harlow.** 2000. Opposing roles of pRB and p107 in adipocyte differentiation. Proc. Natl. Acad. Sci. USA **97:**10826–10831.
7. **de Bruin, A., L. Wu, H. I. Saavedra, P. Wilson, W. Yang, T. J. Rosol, M. Weinstein, M. L. Rosinson, and G. Leone.** 2003. *Rb* function in extraembryonic lineages suppresses apoptosis in CNS of *Rb*-deficient mice. Proc. Natl. Acad. Sci. USA **100:**6546–6551.
8. **Dryja, T. P., J. Rapaport, T. L. McGee, T. M. Nork, and T. L. Schwartz.** 1993.

Molecular etiology of low-penetrance retinoblastoma in two pedigrees. Am. J. Genet. **52:**1122–1128.
9. **Dyson, N.** 1998. The regulation of E2F by pRB-family proteins. Genes Dev. **12:**2245–2262.
10. **Goodrich, D. W., and W. H. Lee.** 1993. Molecular characterization of the retinoblastoma susceptibility gene. Biochim. Biophys. Acta **1155:**43–61.
11. **Gu, W., J. W. Schneider, G. Condorelli, S. Kaushal, V. Mahdavi, and B. Nadal-Ginard.** 1993. Interaction of myogenic factors and the retinoblastoma protein mediates muscle cell commitment and differentiation. Cell **72:**309–324.
12. **Hansen, J. B., R. K. Petersen, C. Jorgensen, and K. Kristiansen.** 2002. Deregulated MAPK activity prevents adipocyte differentiation in fibroblasts lacking the retinoblastoma protein. J. Biol. Chem. **277:**26335–26339.
13. **Harrison, D. J., M. L. Hooper, J. F. Armstrong, and A. R. Clarke.** 1995. Effects of heterozygosity for the Rb-1t19neo allele in the mouse. Oncogene **20:**1615–1620.
14. **Hu, N., A. Gutsmann, D. C. Herbert, A. Bradley, W.-H. Lee, and E. Y. Lee.** 1994. Heterozygous Rb-1 delta 20/+ mice are predisposed to tumors of the pituitary gland with a nearly complete penetrance. Oncogene **9:**1021–1027.
15. **Jacks, T., A. Fazeli, E. M. Schmitt, R. T. Bronson, M. A. Goodell, and R. A. Weinberg.** 1992. Effects of an *Rb* mutation in the mouse. Nature **359:**295–300.
16. **Johnson, L., D. Greenbaum, K. Cichowski, K. Mercer, E. Murphy, E. Schmitt, R. T. Bronson, H. Umanoff, E. Windfried, R. Kucherlapati, and T. Jacks.** 1997. K-*ras* is an essential gene in the mouse with partial functional overlap with N-*ras*. Genes Dev. **11:**2468–2481.
17. **Jones, M. K., and J. H. Jackson.** 1998. Ras-GRF activates Ha-Ras, but not N-Ras or K-Ras 4B, protein *in vivo*. J. Biol. Chem. **273:**1782–1787.
18. **Koera, K., K. Nakamura, K. Nakao, J. Miyoshi, K. Toyoshima, T. Hatta, H. Otani, A. Aiba, and M. Katsuki.** 1997. K-Ras is essential for the development of the mouse embryo. Oncogene **15:**1151–1159.
19. **Kratzke, R. A., G. A. Otterson, A. Hogg, A. B. Coxon, J. Geradts, J. K. Cowell, and F. J. Kaye.** 1994. Partial inactivation of RB product in a family with incomplete penetrance of familial retinoblastoma and benign retinal tumors. Oncogene **9:**1321–1326.
20. **Lasorella, A., M. Noseda, M. Beyna, and A. Iavarone.** 2000. Id2 is a retinoblastoma protein target and mediates signalling by Myc oncoproteins. Nature **407:**592–598.
21. **Lee, E. Y.-H. P., C.-Y. Chang, N. Hu, Y.-C. J. Wang, C.-C. Lai, K. Herrup, W.-H. Lee, and A. Bradley.** 1992. Mice deficient for Rb are nonviable and show defects in neurogenesis and haematopoiesis. Nature **359:**288–294.
22. **Lee, K. Y., M. H. Ladha, C. McMahon, and M. E. Ewen.** 1999. The retinoblastoma protein is linked to the activation of Ras. Mol. Cell. Biol. **19:**7724–7732.
23. **Leone, G., J. DeGregori, R. Sears, L. Jakoi, and J. R. Nevins.** 1997. Myc and Ras collaborate in inducing accumulation of active cyclin E/Cdk2 and E2F. Nature **387:**422–426.
24. **Lohmann, D. R., B. Brandt, W. Hopping, E. Passarge, and B. Horsthemke.** 1994. Distinct RB1 gene mutations with low penetrance in hereditary retinoblastoma. Hum. Genet. **94:**349–354.
25. **MacPherson, D., J. Sage, D. Crowley, A. Trumpp, R. T. Bronson, and T. Jacks.** 2003. Conditional mutation of Rb causes cell cycle defects without apoptosis in the central nervous system. Mol. Cell. Biol. **23:**1044–1053.
26. **Mittnacht, S., H. Paterson, M. F. Olson, and C. J. Marshall.** 1997. Ras signalling is required for inactivation of tumour suppressor pRb cell-cycle control protein. Curr. Biol. **7:**219–221.
27. **Novitch, B. G., G. J. Mulligan, T. Jacks, and A. B. Lassar.** 1996. Skeletal muscle cells lacking the retinoblastoma protein display defects in muscle gene expression and accumulate in S and G_2 phases of the cell cycle. J. Cell Biol. **135:**441–456.
28. **Novitch, B. G., D. B. Spicer, P. S. Kim, W. L. Cheung, and A. B. Lassar.** 1999. pRb is required for MEF2-dependent gene expression as well as cell-cycle arrest during skeletal muscle differentiation. Curr. Biol. **9:**449–459.
29. **Onadim, Z., A. Hogg, P. N. Baird, and J. K. Cowell.** 1992. Oncogenic point mutations in exon 20 of the RB1 gene in families showing incomplete penetrance and mild expression of the retinoblastoma phenotype. Proc. Natl. Acad. Sci. USA **89:**6177–6181.
30. **Peeper, D. S., T. M. Upton, M. H. Ladha, E. Neuman, J. Zalvide, R. Bernards, J. A. DeCaprio, and M. E. Ewen.** 1997. Ras signalling linked to the cell-cycle machinery by the retinoblastoma protein. Nature **386:**177–181.
31. **Raptis, L., H. L. Brownell, M. J. Corbley, K. W. Wood, D. Wang, and T. Haliotis.** 1997. Cellular *ras* gene activity is required for full neoplastic transformation by the large tumor antigen of SV40. Cell Growth Differ. **8:**891–901.
32. **Riley, D. J., A. Y. Nikitin, and W.-H. Lee.** 1996. Adenovirus-mediated retinoblastoma gene therapy suppresses spontaneous pituitary melanotroph tumors in $Rb^{+/-}$ mice. Nat. Med. **2:**1316–1321.
33. **Saavendra, H. I., L. Wu, A. de Bruin, C. Timmers, T. J. Rosol, M. Weinstein, M. L. Robinson, and G. Leone.** 2002. Specificity of E2F1, E2F2 and E2F3 in mediating phenotypes induced by loss of Rb. Cell Growth Differ. **13:**215–225.
34. **Sellers, W. R., B. G. Novitch, S. Miyake, A. Heith, G. A. Otterson, F. J. Kaye, A. B. Lassar, and W. G. J. Kaelin.** 1998. Stable binding to E2F is not required for the retinoblastoma protein to activate transcription, promote differentiation, and suppress tumor growth. Genes Dev. **12:**96–106.
35. **Singh, P., S. W. Chan, and W. Hong.** 2001. Retinoblastoma protein is functionally distinct from its homologues in affecting glucocorticoid receptor-mediated transcription and apoptosis. J. Biol. Chem. **276:**13762–13770.
36. **Singh, P., J. Coe, and W. Hong.** 1995. A role for the retinoblastoma protein in potentiating transcriptional activation of the glucocorticoid receptor. Nature **374:**562–565.
37. **Takahashi, C., N. Akiyama, T. Matsuzaki, S. Takai, H. Kitayama, and M. Noda.** 1996. Characterization of a human MSX-2 cDNA and its fragment isolated as a transformation suppressor gene against v-Ki-ras oncogene. Oncogene **12:**2137–2146.
38. **Takahashi, C., R. T. Bronson, M. Socolovsky, B. Contreras, K. Y. Lee, T. Jacks, M. Noda, R. Kucherlapati, and M. E. Ewen.** 2003. *Rb* and N-*ras* function together to control differentiation in the mouse. Mol. Cell. Biol. **23:**5256–5268.
39. **Tenen, D. G.** 2003. Disruption of differentiation in human cancer: AML shows the way. Nat. Rev. Cancer **3:**89–101.
40. **Thomas, D. M., S. A. Carty, D. M. Piscopo, J.-S. Lee, W.-F. Wang, W. C. Forrester, and P. W. Hinds.** 2001. The retinoblastoma protein acts as a transcriptional coactivator required for osteogenic differentiation. Mol. Cell **8:**303–316.
41. **Tsai, K. Y., Y. Hu, K. F. Macleod, D. Crowley, L. Yamasaki, and T. Jacks.** 1998. Mutation of *E2f-1* suppresses apoptosis and inappropriate S phase entry and extends survival of *Rb*-deficient mouse embryos. Mol. Cell **2:**293–304.
42. **Whitaker, L. L., H. Su, R. Baskaran, E. S. Knudsen, and J. Y. J. Wang.** 1998. Growth suppression by an E2F-binding-defective retinoblastoma protein (RB): contribution from the RB C pocket. Mol. Cell. Biol. **18:**4032–4042.
43. **White, A., and S. Gibson.** 1998. ACTH precursors: biological significance and clinical relevance. Clin. Endocrinol. (Oxford) **48:**251–255.
44. **Williams, B. O., L. Remington, D. M. Albert, S. Mukai, R. T. Bronson, and T. Jacks.** 1994. Cooperative tumorigenic effects of germline mutations in *Rb* and *p53*. Nat. Genet. **7:**480–484.
45. **Wu, L., A. de Bruin, H. I. Saavedra, M. Starovic, A. Trimboli, Y. Yang, J. Opavska, P. Wilson, J. C. Thompson, M. C. Ostrowski, T. J. Rosol, L. A. Woollett, M. Weinstein, J. C. Cross, M. L. Rosinson, and G. Leone.** 2003. Extra-embryonic function of Rb is essential for embryonic development and viability. Nature **421:**942–947.
46. **Yamasaki, L., R. Bronson, B. O. Williams, N. J. Dyson, E. Harlow, and T. Jacks.** 1998. Loss of E2F-1 reduces tumorigenesis and extends the lifespan of $Rb1^{+/-}$ mice. Nat. Genet. **18:**360–364.
47. **Zacksenhaus, E., Z. Jiang, D. Chung, J. D. Marth, R. A. Phillips, and B. L. Gallie.** 1996. pRb controls proliferation, differentiation, and death of skeletal muscle cells and other lineages during embryogenesis. Genes Dev. **10:**3051–3064.
48. **Ziebold, U., E. Y. Lee, R. T. Bronson, and J. A. Lees.** 2003. E2F3 loss has opposite effects on different pRB-deficient tumors, resulting in suppression of pituitary tumors but metastasis of medullary thyroid carcinomas. Mol. Cell. Biol. **23:**6542–6552.
49. **Ziebold, U., T. Reza, A. Caron, and J. A. Lees.** 2001. E2F3 contributes both to the inappropriate proliferation and to the apoptosis arising in *Rb* mutant embryos. Genes Dev. **15:**386–391.